

Article

Removal of Fe(III), Cd(II), and Zn(II) as Hydroxides by Precipitation–Flotation System

Leonor Zapién Serrano ¹, Noemí Ortiz Lara ^{1,2} , Rafael Ríos Vera ³ and Diana Cholico-González ^{1,2,*} 

¹ Instituto de Investigación en Metalurgia y Materiales, Universidad Michoacana de San Nicolás de Hidalgo, Morelia 58030, Mexico; dark.angel_5891@hotmail.com (L.Z.S.); noemi.ortiz@umich.mx (N.O.L.)

² Consejo Nacional de Ciencia y Tecnología, Mexico City 03940, Mexico

³ Facultad de Química, Universidad Autónoma de Querétaro, Santiago de Querétaro 76010, Mexico; rafael.rios.vera@uaq.mx

* Correspondence: diana.cholico@umich.mx; Tel.: +52-(443)-322-35-00 (ext. 4037)

Abstract: In this paper, a combined precipitation–flotation system is proposed for the removal of Fe(III), Zn(II), and Cd(II) as hydroxides. The efficiency of precipitation, as a function of pH, metal ion concentration, and dosage of the precipitating agent as the main variables, was evaluated. The results showed that 99% efficiency was attained from a mixture solution containing the three metal ions in sulfate media at pH 10.3 after 15 min of treatment. The sedimentation behavior showed that a larger precipitate facilitated solid/liquid separation at 30 min. The characterization of precipitates was performed by X-ray diffraction (XRD) identifying iron, zinc, and cadmium oxides; hydroxides; and sodium sulfate. For the flotation, a 20 mg/L solution of dodecylamine (DDA) was used as a collector. Such a solution allowed for the removal of 76% of precipitates in concentrate. An increase in the collector concentration diminished the float percentage due to the micelle formation and low adsorption of the collector on the surface of the precipitate. The results provide evidence of the effectivity of the removal of metal ions by the combined precipitation–flotation system as an alternative for the treatment of acid mine drainage (AMD) in less time in comparison with a sedimentation stage.

Keywords: hydroxides; precipitation; flotation; iron(III); zinc(II); cadmium(II)



Citation: Serrano, L.Z.; Lara, N.O.; Vera, R.R.; Cholico-González, D. Removal of Fe(III), Cd(II), and Zn(II) as Hydroxides by Precipitation–Flotation System. *Sustainability* **2021**, *13*, 11913. <https://doi.org/10.3390/su132111913>

Academic Editor: Gujie Qian

Received: 30 August 2021

Accepted: 26 October 2021

Published: 28 October 2021

Publisher's Note: MDPI stays neutral with regard to jurisdictional claims in published maps and institutional affiliations.



Copyright: © 2021 by the authors. Licensee MDPI, Basel, Switzerland. This article is an open access article distributed under the terms and conditions of the Creative Commons Attribution (CC BY) license (<https://creativecommons.org/licenses/by/4.0/>).

1. Introduction

In Mexico, 4.4% of the consumption of water is related to industrial applications (including the mining industry), demanding direct exploitation of rivers, streams, lakes, or aquifers [1]. In the mining industry, large volumes of water are required in different areas of the comminution and concentration process [2]. For instance, in the gold industry, a tonne of water is used for each tonne of ore, whereas in the flotation process, 3–4 tonnes for a tonne of ore is required [3,4]. The water used in these processes is known as acid mine drainage (AMD) due to its low pH and high metal ion and sulfate concentrations. These characteristics are induced by sulfide mineral oxidation and hydrolysis reactions [5,6]. Fe, Cd, Zn, Cu, Mn, Pb, Ni, and Al are the most common metals found in AMD besides metalloids such as As, and their concentrations are related to the type of mineral processed [7–9]. The solubility of the metal ions in acidic media facilitates its dispersion, which in turn represents a detrimental effect on the environment and health [8,10]. The importance of the treatment of AMD lies in the inherent need for the removal of heavy metal ions, which can be toxic both for health and the environment, in addition to the option of reusing water, reducing consumption. Some studies suggested that the reuse of water can have important implications in other industries, as well [11].

Physical, chemical, and biological methods have been developed for AMD treatment [12–15]. Among these, chemical precipitation has advantages over other procedures,

such as short reaction time, high recovery efficiency, good selectivity, and minimal operational management [10]. Furthermore, the technique allows for the removal of metal ions by the addition of a reagent, which in turn determines the type of solid formed, either sulfides or hydroxides [16,17]. Hydroxide precipitation is often performed by adding CaO, Ca(OH)₂, or NaOH as reagents [12,18,19]. Variables such as metal ion concentrations, pH, and the nature of the precipitating agent directly influence the efficiency of the process, besides affecting the characteristics acquired by the solid particle. The main drawback of chemical precipitation is related to the solid–liquid separation since a portion of the precipitate remains suspended, hindering the solid recovery [17]. Because of that, the long sedimentation time which is needed to separate the water and precipitate is the main constraint. To address this, froth flotation, a well-known technique in the mining industry to concentrate ores through the separation of solids of a different nature (hydrophilic or hydrophobic) by adding a compound named a collector [20,21], has been proposed. Compounds such as sodium oleate, potassium ethyl xanthate, dodecylamine, and sodium dodecyl sulfate have been used as collectors for the recovery of precipitates [21–24]. Even more, some specialized techniques, such as precipitation–flotation, ionic flotation, reverse flotation, or adsorption flotation, represent alternatives to the removal of metal ions [23,25–27]. Nevertheless, a combined system of precipitation–flotation offers the possibility of performing both an efficient removal of metal ions and the recovery of solids. To achieve this, the nature of precipitates, composition, and surface charge must be considered [28,29]. Recently, ion flotation was employed to remove metal ions such as copper, lead, zinc, cadmium, and nickel from a low-concentration aqueous solution. The collector used was sodium dodecyl sulfate reaching efficiencies of 83–89% at pH 9 [24]. Nevertheless, ion flotation presented a high dependence of chemical speciation and was favored at alkaline pH values similar to chemical precipitation. The application of reverse flotation for the removal of iron oxides using dodecylamine as a collector in the presence of multivalent cations, achieving efficiencies of 85%, has been reported [30]. Regarding precipitation–flotation, recently, the interaction of Fe(III) as a controller of precipitate and hummics chelating as a precipitant agent was evaluated. Precipitation efficiency for Cu(II), Pb(II), and Zn(II) was enhanced to a level above 94% [31]. Subsequently, the same authors [32] combined Fe(III) and CTAB (cetyl trimethyl ammonium bromide) to increase particle size and to achieve a coarser and lighter structure. The final precipitate flocs are hard to be broken up, easy to be recovered, and efficient to be recovered by froth flotation, reaching a removal of 98–99%. The precipitation–flotation system has been also investigated for the extraction of other metal ions such as Rb(I) and Cs(I) from aqueous solutions using ammonium phosphowolframate as the precipitating agent and CTAB as the collector [33]. According to the authors, the extraction efficiency can reach almost 100% under optimal experimental conditions.

The viability of the precipitation–flotation system depends on determining the optimal conditions for each step. Therefore, providing information to improve the solid–liquid separation and to assure the composition of the precipitates will allow further control and assessing the possibility of recovering valuable metals [5,8]. Most references focus on precipitation efficiency, leaving aside the sedimentation, characterization, and further recovery of solids. On the other hand, characterization of the precipitates and tailings after flotation is limited. Complete knowledge of the precipitation–flotation system will offer the mining industry an alternative for the efficient treatment of AMD that in the long term contributes to more sustainable mining, reducing its environmental impact in terms of water consumption and the high heavy metal ion concentration in wastewater [34].

This research aim was to systematically evaluate the chemical precipitation of Fe(III), Cd(II), and Zn(II) as hydroxides and the evaluation of the flotation of precipitates by the dodecylamine (DDA) as a collector. A characterization of precipitates, concentrates and tailing after flotation was performed.

2. Materials and Methods

2.1. Reagents

All reagents were analytical grade (purity $\geq 98\%$). Solutions containing metal ions were prepared by dissolving the appropriate amount of the salts ZnSO_4 (J.T. Baker), $\text{Fe}_2(\text{SO}_4)_3$, and CdSO_4 (Q. Meyer) in distilled water with a fixed sulfate content given by 0.1 mol/L H_2SO_4 (Q. Meyer) to simulate an AMD. The dodecylamine (DDA) was supplied by Fluka Analytical and was used as a collector. Fresh solutions of NaOH and HCl (Q. Meyer) were used for pH control.

2.2. Precipitation Experiments

To establish the precipitation conditions, it was necessary to take into account the precipitation reactions for each metal ion. A chemical diagram of the logarithm of solubility as a function of pH was generated using the HYDRA/Medusa software, considering the metal ion concentrations in the precipitation experiments and the entire range of pH [35].

The chemical precipitation was carried out from solutions containing a mixture of the three metal ions at different concentrations. Such solutions, named MS1, MS2, and MS3, are presented in Table 1. Precipitation was performed by adding NaOH as a precipitating agent, evaluating the effect of pH 5.3, 9.0, and 10.3, based on the chemical diagram. Dosage rates of NaOH of 2.5, 5.0, 7.5, and 10.0 mL/min were evaluated at pH 10.3 to assure the precipitation of the three metal ions. In all cases, the time of precipitation was 15 min using 2 L of mixture solution and was maintained at room temperature under constant stirring (150 rpm) unless otherwise stated. pH was adjusted to the desired value by adding a fresh solution of NaOH or HCl and was monitored by a Hanna Potentiometer HI2550. The instrument, with a pH combined glass electrode, was previously calibrated using pH 7, 4, and 10 buffer solutions (Hanna Instruments).

Table 1. Concentrations of metal ions in mixed solutions.

Mixed Solution	Metal Ion Concentration $\times 10^{-3}$, mol/L		
	Fe(III)	Zn(II)	Cd(II)
MS1	1.29 \pm 0.02	1.70 \pm 0.02	0.93 \pm 0.01
MS2	6.76 \pm 0.19	7.79 \pm 0.04	4.57 \pm 0.04
MS3	13.40 \pm 0.19	15.48 \pm 0.08	9.03 \pm 0.06

After precipitation, all samples were vacuum filtered through a 0.22 μm membrane (GSWP4700, Merck Millipore Ltd.) and the residual solution was acidified with 2 mol/L HCl to avoid further precipitation. The recovered solids were dried in an oven at 105 $^\circ\text{C}$ for 2 h and stored in a desiccator until their characterization.

Quantification of the metal ions concentration, at the initial and final conditions, was performed by Atomic Absorption Spectroscopy in a Perkin-Elmer 3100 equipment. Calibration was brought out from 1000 mg/L standard solutions containing Fe, Zn, or Cd (Sigma-Aldrich).

Mass balances for the different metal ions were obtained with the following equation:

$$C_0 \cdot V_0 = C_f \cdot V_f + M(\text{III or II})_{\text{precipitated}} \quad (1)$$

where C_0 and C_f are the initial and residual concentrations of the different metal ions (mol/L), respectively; V_0 and V_f are the initial and residual volume of solutions (L), respectively; and $M(\text{III or II})$ represents the mass of metal ions such as Fe(III), Cd(II), or Zn(II) that were precipitated. Considering Equation (1), the precipitation efficiency (PE) can be calculated as:

$$PE (\%) = \frac{C_0 \cdot V_0 - C_f \cdot V_f}{C_0 \cdot V_0} \cdot 100 \quad (2)$$

Sedimentation behavior after precipitation at pH 10.3 was determined from the MS1, MS2, and MS3 solutions, with dosage rates of 2.5, 5.0, 7.5, and 10.0 mL/min of NaOH as the precipitant agent. After precipitation, the slurry was transferred to a 1 L Imhoff cone

and was treated according to the standard method [36]. Sediment volume expressed in mL was plotted as a function of time for each solution. Solids were then filtered and dried as was described previously. To obtain the particle size distribution, the dry precipitates were screened through 16, 35, 60, 120, and 325 mesh sieves (Tyler Standard) in a vibratory sieve shaker Retsch AS-200 for 1 min. The particle size distribution was calculated from the retained fraction on each sieve.

2.3. Flotation Test

Flotation tests were developed by obtaining the precipitates from 125 mL of MS1 or MS3 solutions at pH 10.3. Subsequently, the precipitates were conditioned for 10 min, adding dodecylamine (DDA) as a collector. The conditioned slurry was later transferred into a Hallimond tube and kept for 10 min under a constant flow of 20 mL/min of N₂ to promote the flotation of solids. A scheme describing the complete process of precipitation–flotation is presented in Figure 1.

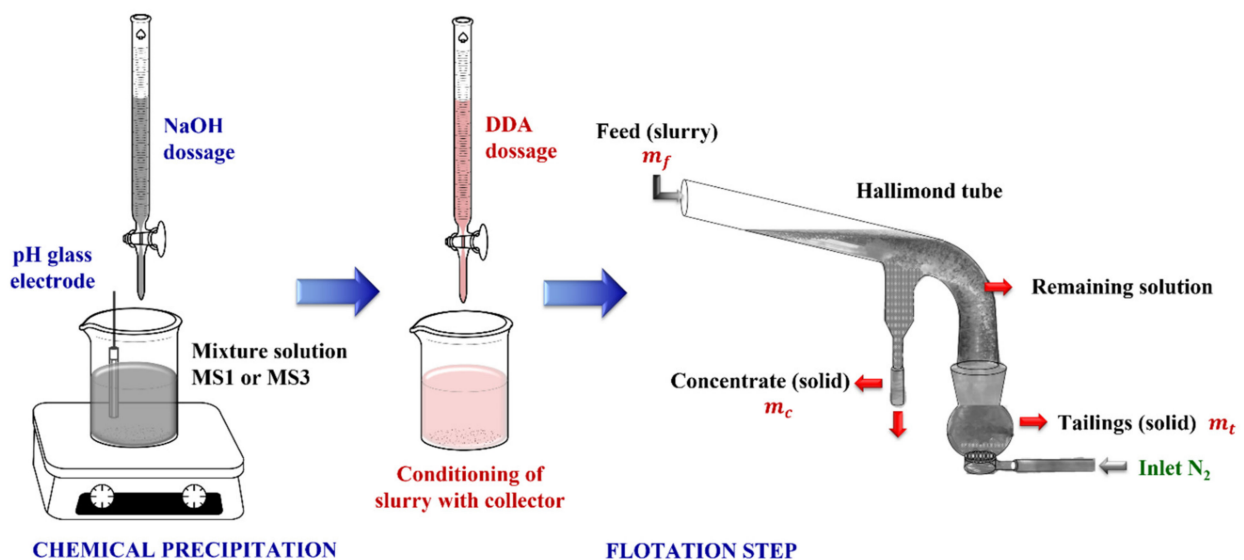


Figure 1. Scheme of the precipitation–flotation system.

After flotation, the concentrate (floated mass, m_c) and tailings (non-floated mass, m_t) were recovered, dried as described above, and weighed in an AB135 Mettler-Toledo analytical balance. Subsequently, they were stored in a desiccator until characterization.

The flotation efficiency was calculated as follows:

$$\% \text{ Flotation efficiency} = \frac{m_c}{m_f} \times 100 \quad (3)$$

where m_f is the mass of the precipitate in the feed (mg) and m_c corresponds to the mass of the precipitate in the concentrate (mg). The m_f value can be obtained from the sum of m_c and m_t .

2.4. Characterization of Samples

The recovered solids from precipitation and flotation experiments were analyzed in a D8 Advance Davinci Diffractometer (Bruker) with Cu-K α radiation and Ni filter. Data were recorded in a range 2 Theta of 10° to 90° with a step size of 0.02° and 0.6 sec. Indexation of the peaks was performed with the JCPDS cards of the DIFRAC.EVA software database.

The zeta potential (ζ) values of precipitates obtained from MS1, MS2, and MS3 solutions were measured in a ZetaProbe Analyzer (Colloidal Dynamics) using 5 g of the sample

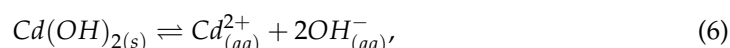
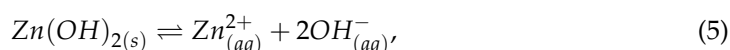
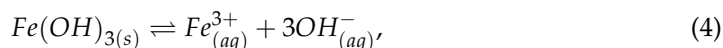
at 1.8% of solids in a KCl 1×10^{-3} mol/L solution to assure a constant ionic strength at pH values between 4 and 11.

3. Results and Discussion

3.1. Chemical Precipitation

3.1.1. Solubility of Precipitates

Formation of Fe(III), Zn(II), and Cd(II) hydroxides involve the chemical equilibrium depicted in the following reactions (4)–(6) that are highly dependent on metal ion concentration and pH value:



Considering these reactions, an increase in hydroxide concentration $[OH^{-}]$ enhances the metal hydroxide formation because the chemical equilibrium is displaced in the direction of the $Fe(OH)_{3(s)}$, $Zn(OH)_{2(s)}$, and $Cd(OH)_{2(s)}$ formation. Figure 2 shows a logarithmic diagram of the solubility of Fe(III), Zn(II), and Cd(II), in terms of pH for 1.29×10^{-3} , 1.70×10^{-3} , and 0.93×10^{-3} mol/L, respectively, in the presence of 0.1 mol/L of SO_4^{2-} , conditions that correspond to the MS1.

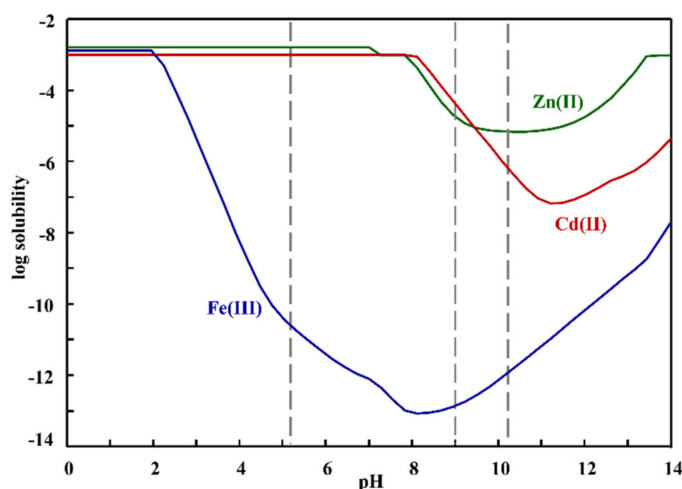


Figure 2. Logarithm of solubility of metal ions vs pH diagram. $[Fe(III)] = 1.29 \times 10^{-3}$ mol/L, $[Zn(II)] = 1.70 \times 10^{-3}$ mol/L, $[Cd(II)] = 0.93 \times 10^{-3}$ mol/L, and $[SO_4^{2-}] = 0.1$ mol/L.

At acid pH values (0–2), the three metal ions are soluble. Fe(III) sharply decreases its solubility due to its precipitation as $Fe(OH)_{3(s)}$ according to the reaction (4). From pH 2 until pH around 8, it reaches a minimum value of solubility. The solubility of Zn(II) and Cd(II) diminishes around pH 7.5 and 8, respectively, related to reactions (5) and (6). Between pH 8 and 11, the lowest solubility of Zn(II) is observed, whereas for the Cd(II), a pH of 11 is required. Although the solubility is increased again by raising pH above 8, for the case of Fe(III) or Cd(II), this does not represent a loss in efficiency because the solubility does not exceed 10^{-8} or 10^{-6} mol/L, respectively, even at pH 14. This means that the final concentration is several orders of magnitude less than the initial one. The solubility of Zn(II), unlike the other metal ions, can be increased above pH 11, until the complete redissolution of precipitate is achieved, affecting the efficiency notably.

Based on the previous diagram, three conditions of pH were selected (5.3, 9.0, and 10.3, as indicated with dotted lines in Figure 2) to evaluate the precipitation of Fe(II), Zn(II), and Cd(II) from mixture solutions MS1, MS2, and MS3. At pH 5.3, it is possible to precipitate the Fe(III) without Zn(II) or Cd(II), whereas at pH 9.0, the precipitation of Fe(III) and Zn(II)

can be reached. Finally, at pH 10.3, the hydroxide formation from the three metal ions can be obtained, avoiding the redissolution of $Zn(OH)_{2(s)}$.

3.1.2. Effect of pH and Initial Concentration for Mixed Metal Ions Solutions on Precipitation Efficiency

Figure 3a shows the simultaneous precipitation efficiency of Fe(III), Zn(II), and Cd(II) at different pH values from MS1. The Fe(III) precipitation was higher than 99% at all pH conditions evaluated in the presence of Cd(II) and Zn(II). At pH 5.3, a slight precipitation of Cd(II) and Zn(II) (<2%) was obtained, which is in agreement with the diagram of Figure 2. At pH 9.0, the precipitation efficiency for Zn(II) was superior to 99%, while Cd(II) reached only 40%. The complete precipitation of three metal ions was reached at pH 10.3 from MS1.

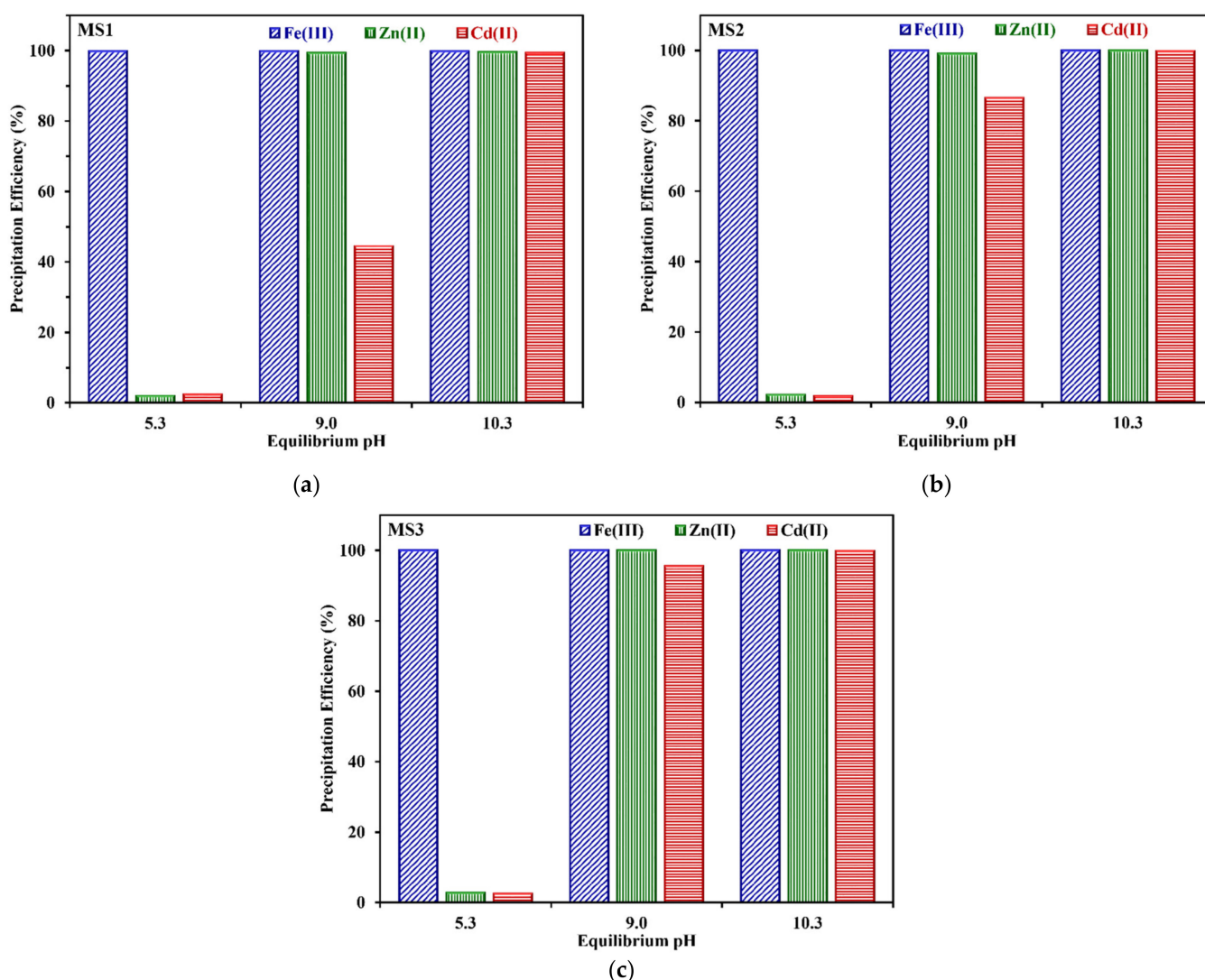


Figure 3. Effect of pH and initial concentration on precipitation efficiency from mixed metal ion solution: (a) MS1; (b) MS2; (c) MS3. Precipitation time: 15 min.

Figure 3b,c report the precipitation efficiency of metal ions from MS2 and MS3, respectively. In the case of Fe(III), precipitation efficiency remained at 99% when the initial concentration was increased from 1.29×10^{-3} to 13.40×10^{-3} mol/L. Results of Zn(II) precipitation efficiency for the MS2 and MS3 were higher than 99% at pH 9.0 and 10.3. The same behavior was observed for the precipitation efficiency of Cd(II). The precipitation behavior from mixed solutions corresponds to that found in single metal ion solutions. At these conditions, OH^- concentration in the system is enough to react with the metal

ions and form the hydroxides species. An increase in the initial concentration values improves the precipitation efficiency at the same pH. This effect can be explained by the high concentration of metal ions and sulfates in media, which induces an increase in the ionic force, and then the solubility of hydroxides diminishes [17]. Therefore, an increase in initial concentration promotes the hydroxide formation to begin at lower pH values. Similarly, results about the precipitation in the presence of metal ions were reported [18,37]. For an efficient removal of the metal ions from a mixture solution, a pH of 10.3 is appropriate. Nevertheless, it is worth noting that it is possible to achieve selective precipitation, removing Fe(III) at pH 5.3, Zn(II) at pH 9.0, and Cd(II) at pH 10.3.

3.1.3. Effect of Dosage Rate NaOH on Settling Behavior and Particle Size

To evaluate the characteristics of the precipitates obtained from the mixed metal ion solutions, the sedimentation behavior and the particle size were analyzed. Figure 4a shows the sedimentation behavior of precipitates from MS1. For all dosage rates, an initial rapid sedimentation stage was observed, followed by a slower hindered stage. Finally, an increase in the dosage rate slightly increased the sedimentation velocity, reaching the compression zone after 30 min.

Figure 4b,c show the effect of the dosage rate on the settling behavior of precipitates from MS2 and MS3, respectively. Both figures show that the sedimentation rate was lower in comparison with MS1, Figure 4a. A continuous hindered sedimentation stage was observed from the first minutes of treatment, induced by the higher solid concentrations [38]. A higher sedimentation volume was obtained for the largest solid concentration (sludge MS3) and the compression stage was reached after 45 min. These results are coherent with those previously reported [39]. The initial concentration of the metal ion has a notable effect on the sedimentation rate, being higher when the initial concentration is lower (MS1). In this case, the compression stage is quickly achieved due to the low solid content. The fast sedimentation rate for all precipitates is related to the presence of iron hydroxide that is commonly used as a flocculant, promoting, in turn, a fast solid–liquid separation.

Sedimentation behavior is also affected by the particle size of the precipitates. Figure 4d displays the particle size distribution of the precipitates formed from MS1. A dosage rate of the precipitating agent between 2.5–7.5 mL/min promotes particle sizes in a wide range (45–1000 μm). However, a somewhat higher particle size (250–1000 μm) was obtained for 10 mL/min. According to Stoke's law, the largest particles are settled first [40] and, therefore, the rapid sedimentation rate observed in Figure 4a is related to the particle size of precipitates. A shift towards larger sizes in the distribution was observed for precipitate from MS2 (Figure 4e). This phenomenon is related to an increase in the initial concentration, during which the relative saturation of the solution augments and the particle growth is favored. Similar behavior is observed for the precipitates from MS3 (Figure 4f). Figure 4e,f show a bimodal particle size distribution that can be attributed to the fact that the smaller particles are rearranged seeking to minimize the surface area, forming larger particles. The results demonstrated the suitable properties of precipitates to reach sedimentation. However, solid–liquid separation is needed even when the precipitates are sedimented. Characterization of precipitates was conducted to establish composition and surface charge of the particles.

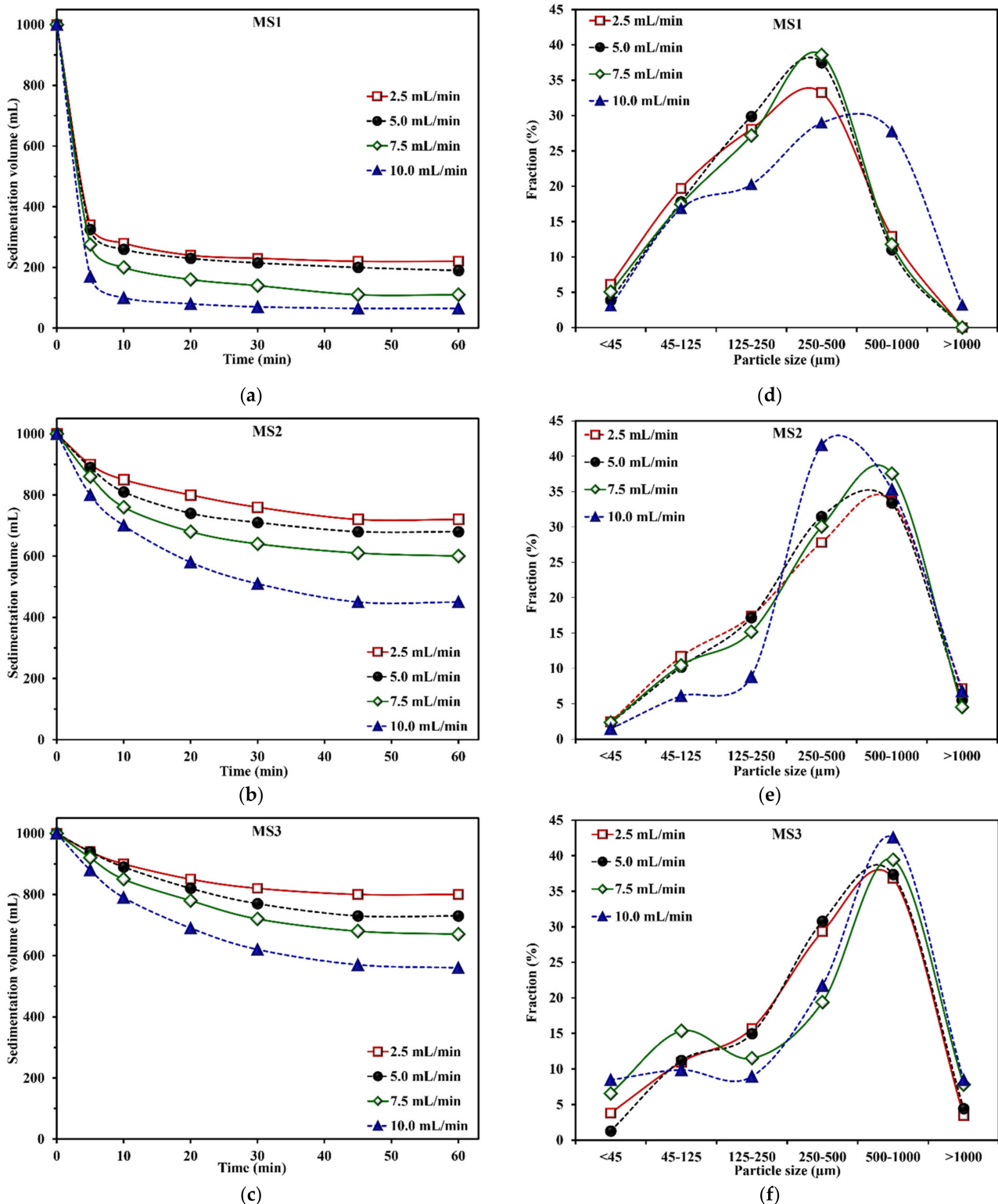


Figure 4. Sedimentation behavior and particle size of precipitates. (a,d) MS1; (b,e) MS2; (c,f) MS3 as a function of dosage rate of NaOH. Precipitation time: 15 min.

3.1.4. Characterization of Precipitates

The results of XRD analysis for the obtained solid precipitates at pH 10.3 from MS1, MS2, and MS3 are shown in Figure 5. The diffraction pattern of the precipitate from MS1 (Figure 5a) shows a diffuse peak around 13° related to the low crystallinity of iron species

and induced by the aggregation of ferrihydrite $\text{Fe}(\text{OH})_3$ at $\text{pH} > 7.5$ due to van der Waals forces [41]. The crystallinity of iron precipitates is strongly influenced by the presence of sulfates during precipitation, slowing the transformation of amorphous to crystalline solid [42]. Other species found in the precipitates correspond to zinc oxide, ZnO (PDF 00-021-1486). The formation of zinc oxide, ZnO , implies the precipitation of amorphous $\text{Zn}(\text{OH})_2$, which, once dry at room temperature, crystallizes as the oxide identified in the diffractograms [43,44]. Olivera [45] associated the same species in the precipitation with NaOH at $\text{pH} 10.5$. The cadmium was precipitated mainly as cadmium hydroxide, $\text{Cd}(\text{OH})_2$ (PDF 04-018-0813), and cadmium oxide, CdO (PDF 00-039-1221). Unlike $\text{Zn}(\text{OH})_2$, $\text{Cd}(\text{OH})_2$ is more stable [44], remaining as this specie in the precipitate. Some signals can also be assigned to sodium sulfate, Na_2SO_4 (PDF 00-001-0990). This solid is present as a by-product of metal ion precipitation with a strong base, NaOH . Its formation is performed by the following reaction:

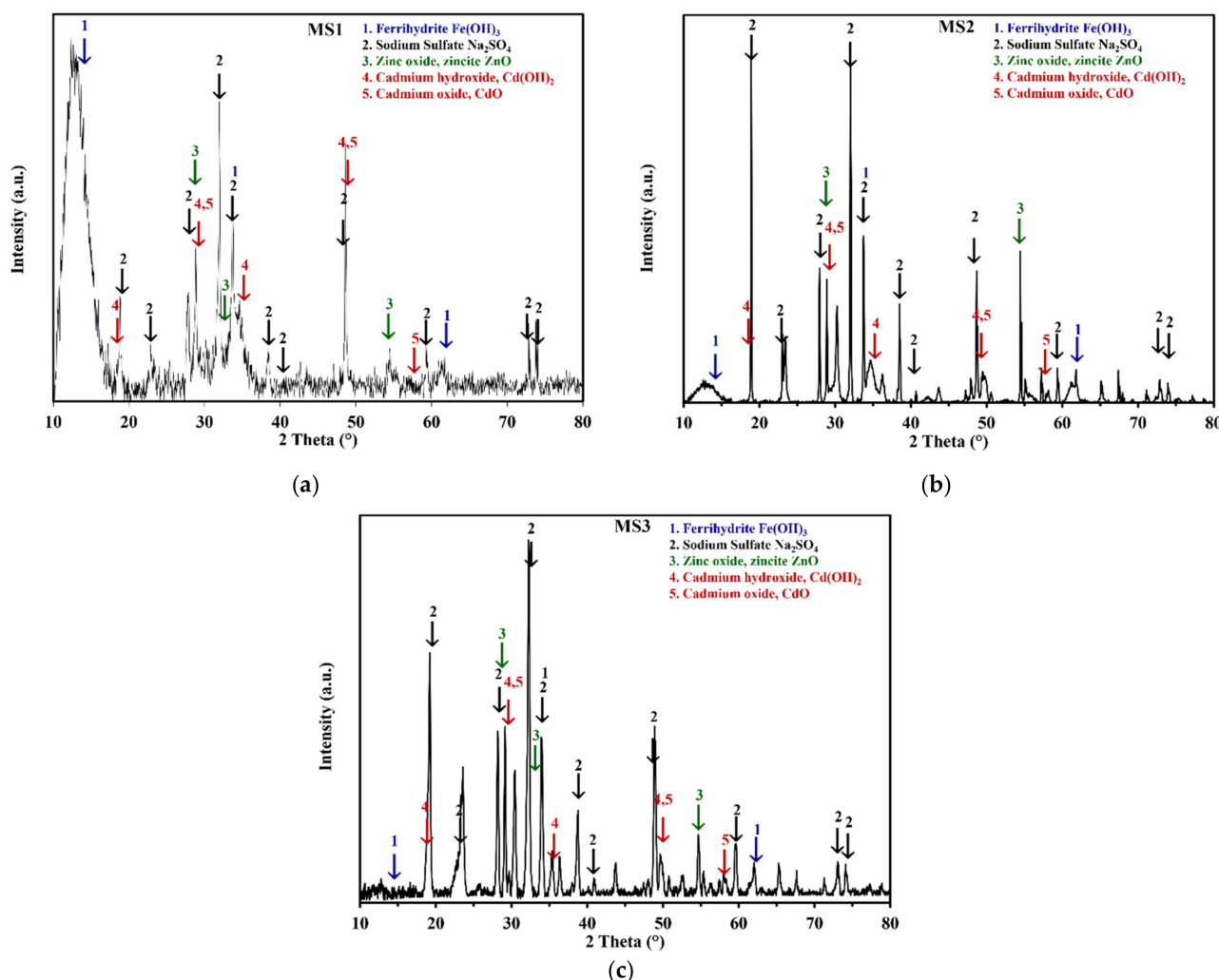
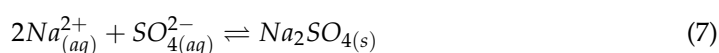


Figure 5. X-ray diffraction patterns of precipitates from mixed metal ions solution: (a) MS1; (b) MS2; (c) MS3.

The presence of Na_2SO_4 in the precipitate is an indication of a decrease in the concentration of dissolved sulfates, contributing to its removal while the metal ions precipitate [46]. Unlike the use of $\text{Ca}(\text{OH})_2$ or CaO as precipitating agents, the NaOH leads to the formation of a less bulky sludge [47]. Using this agent also improves the efficiency of precipitation

because it possesses a higher capacity for the removal of metal ions [19]. In the XRD patterns from precipitates of MS2 and MS3 (Figure 5b,c), the signals show a higher intensity owing to a greater amount of precipitates.

To establish the surface charge, as it is shown in Figure 6, the zeta potential (ζ) of precipitates was obtained from MS1, MS2, and MS3. The zeta potential value is similar for the three samples, showing a positive charge at acid pH with trends to a zero charge value around pH 10.5. Considering the characterization by XRD of the precipitates, the presence of oxides promotes a positive charge at acid pH values, while a negative zeta potential is observed at basic conditions due to its amphoteric behavior [48]. An increase in the zeta potential value in an acid pH value is related to the redissolution of precipitates of Zn(II) and Cd(II). These remain in the solution and contribute to the positive charge. At a precipitation pH of 10.3, the zeta potential value is close to the point of zero charge (PZC) or slightly negative (MS1).

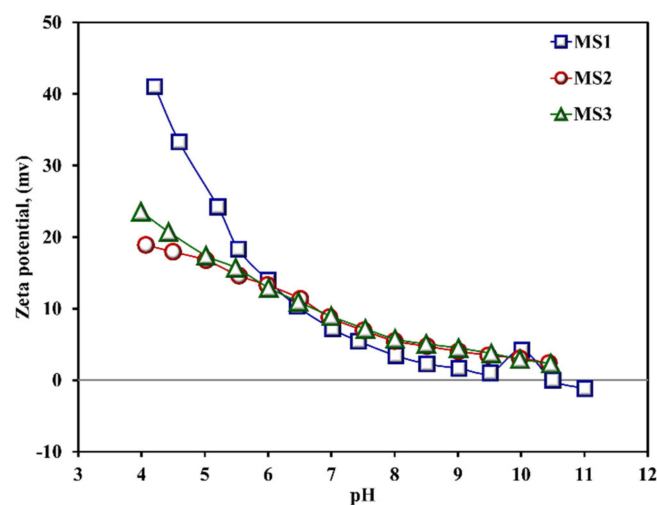


Figure 6. Zeta potential (ζ) of precipitates obtained from MS1, MS2, and MS3 as a function of pH.

3.2. Flotation of Precipitates

3.2.1. Effect of the Mass of the Precipitates and the Dodecylamine Concentration (DDA)

To evaluate the flotation of the precipitates obtained from MS1 and MS3, dodecylamine was added as a collector in a 20 mg/L concentration. The flotation efficiency in the concentrate and tailings is shown in Figure 7a.

The flotation efficiency for MS1 was higher than MS3. In the case of MS3, the amount of concentrate and tailings was practically the same. This result is related to the mass of precipitate obtained, which is higher for MS3 than MS1. The addition of DDA as a collector was not enough because of the large amount of solids inhibiting flotation of precipitates. Then, the effect of DDA concentration on the flotation efficiency was evaluated for the precipitates from MS1 (Figure 7b). An increase in the collector concentration promotes an increase in the floated fraction until, at a maximum of 20 mg/L, it reaches 75.21% floated mass. DDA is a weak electrolyte and its adsorption in the surface is favored at high pH values [49]. At this point, higher flotation efficiencies are promoted by the adsorption of collector molecules at the surface of the precipitate. Above 20 mg/L of DDA, the float percentage shows a decreasing trend, with efficiency values of 74.5 and 69.2% for 50 and 100 mg/L of DDA, respectively. The decrease in the flotation efficiency value can be attributed to the collector concentration used, which was higher than the critical micellar concentration (CMC) of 10^{-4} kmol/m³ or 18.5 mg/L at basic pH conditions [50]. At a concentration level below that of the CMC, the DDA is dissolved and can be adsorbed on the surface of the precipitate. When the concentration is increased above the CMC, the DDA forms aggregates named micelles that limit the amount of the collector that can be absorbed on the precipitate surface. Consequently, the flotation efficiency diminishes when the DDA

concentration is increased. This result leads us to conclude that a 20 mg/L concentration of DDA is the optimal condition to assure the maximum recovery of precipitates.

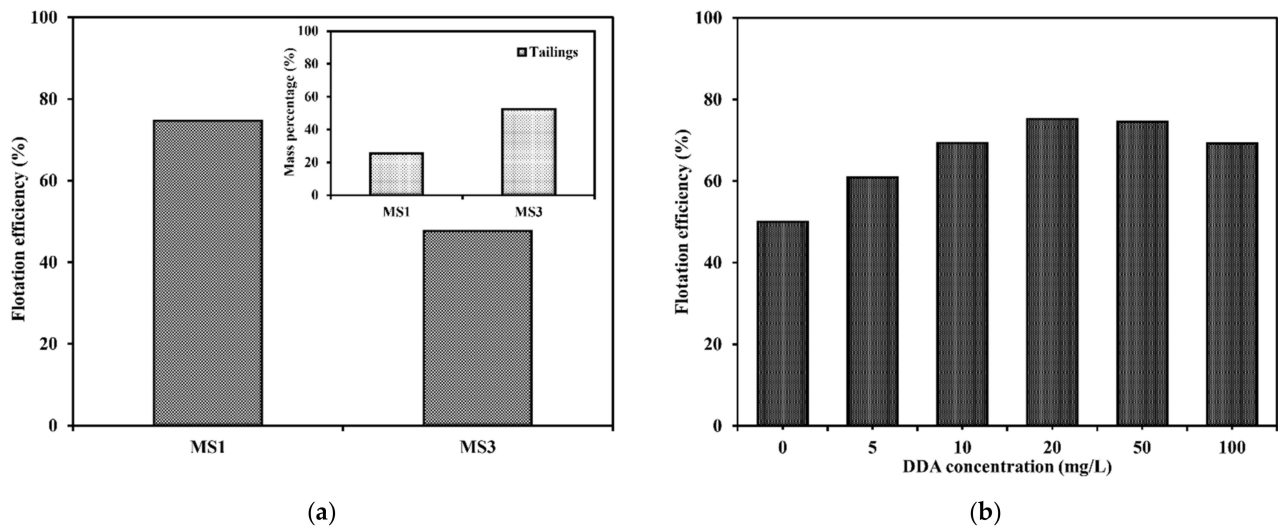


Figure 7. (a) Flotation efficiency for MS1 and MS3 (DDA concentration 20 mg/L). Insert: Mass percentage in tailing for MS1 and MS3. (b) Effect of DDA concentration in flotation efficiency from MS1.

3.2.2. Characterization of Concentrates and Tailings

Once the precipitates were floated, XRD was performed on both the concentrate and the tailings displayed in Figure 8a,b, respectively. In the XRD pattern obtained for the concentrate, there are signals corresponding to the oxides and hydroxides of Fe, Zn, and Cd with higher intensities in comparison with the diffractogram of tailings. Those peaks, which have been attributed to the Na_2SO_4 , were noticeable in both concentrate and tailings, although the absolute intensity is lower in the concentrate than in the tailings. This result shows that the flotation process offers the possibility of a selective separation of the different precipitates.

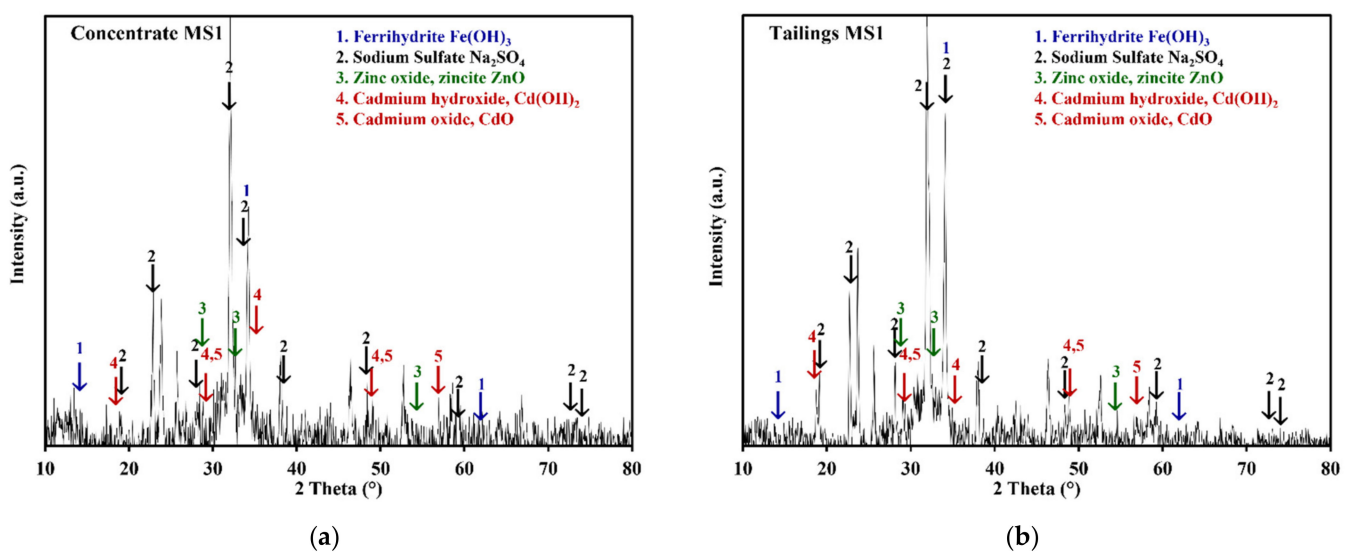


Figure 8. X-ray diffraction patterns of solids from MS1 after flotation: (a) concentrate, (b) tailings.

4. Conclusions

In this study, the precipitation–flotation system was applied successfully to the removal of heavy metal ions as hydroxides. Chemical precipitation of Fe(III), Zn(II), and Cd(II) was evaluated, showing a precipitation efficiency higher than 99% for the three metal ions at a pH value of 10.3. Metal oxides and hydroxides were identified in the precipitates by XRD analysis. The increase in the concentration of the metal ions in the solution promotes an increase in particle size. The DDA was evaluated as a collector to separate the different precipitates by flotation with a 10-min conditioning time. When the collector concentration was increased above the CMC, the flotation efficiency diminished due to the formation of aggregates of the DDA that inhibit its adsorption in the precipitate surface. Characterization by XRD after flotation demonstrated that the metallic phases (metallic oxides and hydroxides) remain preferentially in the concentrate, whilst it was found that the tailings were primarily composed of Na₂SO₄. The results of this work on the precipitation–flotation system contribute to the knowledge of the precipitation, conditioning, flotation, and solid recovery stages. Characterization of the precipitates suggests that the concentrate can have a commercial value while the high removal of metal ions from AMD offers the possibility of the reuse of water. These aspects allow improving the efficient use of water for a more sustainable mining industry.

Author Contributions: Conceptualization, N.O.L. and D.C.-G.; Funding acquisition, D.C.-G.; Investigation, L.Z.S.; Visualization, D.C.-G.; Writing—original draft, L.Z.S.; Writing—review and editing, N.O.L., R.R.V. and D.C.-G. All authors have read and agreed to the published version of the manuscript.

Funding: This research was funded by the Consejo Nacional de Ciencia y Tecnología (CONACYT) through project no. 248126 and by the Ph.D. scholarship no. 369384.

Institutional Review Board Statement: Not applicable.

Informed Consent Statement: Not applicable.

Data Availability Statement: Not applicable.

Acknowledgments: The authors thank the Instituto de Investigación en Metalurgia y Materiales (UMSNH) for the facilities granted and the Consejo Nacional de Ciencia y Tecnología (CONACYT) for financial support to carry out this research.

Conflicts of Interest: The authors declare no conflict of interest.

References

1. Comisión Nacional del Agua. *Estadísticas del Agua en México*; Mexico, 2018.
2. Aitken, D.; Rivera, D.; Godoy-Faúndez, A.; Holzapfel, E. Water Scarcity and the Impact of the Mining and Agricultural Sectors in Chile. *Sustainability* **2016**, *8*, 128. [[CrossRef](#)]
3. Gupta, A.; Yan, D.B.T.-M.P.D.; Second, E.O. (Eds.) Chapter 14—Solid-liquid separation—Thickening. In *Mineral Processing Design and Operations*; Elsevier: Amsterdam, The Netherlands, 2016; pp. 471–506, ISBN 978-0-444-63589-1.
4. Zhai, D.; Feng, B.; Guo, Y.; Zhou, X.; Wang, T.; Wang, H. Settling behavior of tungsten tailings using serpentine as flocculant. *Sep. Purif. Technol.* **2019**, *224*, 304–307. [[CrossRef](#)]
5. Naidu, G.; Ryu, S.; Thiruvengkatachari, R.; Choi, Y.; Jeong, S.; Vigneswaran, S. A critical review on remediation, reuse, and resource recovery from acid mine drainage. *Environ. Pollut.* **2019**, *247*, 1110–1124. [[CrossRef](#)] [[PubMed](#)]
6. Skousen, J.G.; Ziemkiewicz, P.F.; McDonald, L.M. Acid mine drainage formation, control and treatment: Approaches and strategies. *Extr. Ind. Soc.* **2019**, *6*, 241–249. [[CrossRef](#)]
7. Park, I.; Tabelin, C.B.; Jeon, S.; Li, X.; Seno, K.; Ito, M.; Hiroyoshi, N. A review of recent strategies for acid mine drainage prevention and mine tailings recycling. *Chemosphere* **2019**, *219*, 588–606. [[CrossRef](#)]
8. Simate, G.S.; Ndlovu, S. Acid mine drainage: Challenges and opportunities. *J. Environ. Chem. Eng.* **2014**, *2*, 1785–1803. [[CrossRef](#)]
9. Nordstrom, D.K.; Bowell, R.J.; Campbell, K.M.; Alpers, C.N. Challenges in recovering resources from acid mine drainage. In Proceedings of the 13th International Mine Water Association Congress — “Mine Water & Circular Economy — A Green Congress”, Lappeenranta, Finland, 25–30 June 2017.
10. Macingova, E.; Luptakova, A. Recovery of Metals from Acid Mine Drainage. *Chem. Eng. Trans.* **2012**, *28*, 109–114. [[CrossRef](#)]
11. Villamar, C.-A.; Vera-Puerto, I.; Rivera, D.; De la Hoz, F. Reuse and Recycling of Livestock and Municipal Wastewater in Chilean Agriculture: A Preliminary Assessment. *Water* **2018**, *10*, 817. [[CrossRef](#)]

12. Rahman, M.T.; Kameda, T.; Kumagai, S.; Yoshioka, T. Effectiveness of Mg–Al-layered double hydroxide for heavy metal removal from mine wastewater and sludge volume reduction. *Int. J. Environ. Sci. Technol.* **2018**, *15*, 263–272. [[CrossRef](#)]
13. Azimi, A.; Azari, A.; Rezakazemi, M.; Ansarpour, M. Removal of Heavy Metals from Industrial Wastewaters: A Review. *ChemBioEng Rev.* **2017**, *4*, 37–59. [[CrossRef](#)]
14. Moodley, I.; Sheridan, C.M.; Kappelmeyer, U.; Akcil, A. Environmentally sustainable acid mine drainage remediation: Research developments with a focus on waste/by-products. *Miner. Eng.* **2018**, *126*, 207–220. [[CrossRef](#)]
15. Oncel, M.S.; Muhcu, A.; Demirbas, E.; Kobya, M. A comparative study of chemical precipitation and electrocoagulation for treatment of coal acid drainage wastewater. *J. Environ. Chem. Eng.* **2013**, *1*, 989–995. [[CrossRef](#)]
16. Mokone, T.P.; van Hille, R.P.; Lewis, A.E. Effect of solution chemistry on particle characteristics during metal sulfide precipitation. *J. Colloid Interface Sci.* **2010**, *351*, 10–18. [[CrossRef](#)]
17. Wang, L.K.; Vaccari, D.A.; Li, Y.; Shammass, N.K. *Chemical Precipitation BT—Physicochemical Treatment Processes*; Wang, L.K., Hung, Y.-T., Shammass, N.K., Eds.; Humana Press: Totowa, NJ, USA, 2005; pp. 141–197, ISBN 978-1-59259-820-5.
18. Byambaa, M.; Dolgor, E.; Shiomori, K.; Suzuki, Y. Removal and Recovery of Heavy Metals from Industrial Wastewater by Precipitation and Foam Separation Using Lime and Casein. *J. Environ. Sci. Technol.* **2018**, *11*, 1–9. [[CrossRef](#)]
19. Kefeni, K.K.; Msagati, T.A.M.; Mamba, B.B. Acid mine drainage: Prevention, treatment options, and resource recovery: A review. *J. Clean. Prod.* **2017**, *151*, 475–493. [[CrossRef](#)]
20. Zhang, X.; Gu, X.; Han, Y.; Parra-Álvarez, N.; Claremboux, V.; Kawatra, S.K. Flotation of Iron Ores: A Review. *Miner. Process. Extr. Metall. Rev.* **2021**, *42*, 184–212. [[CrossRef](#)]
21. Matis, K.A.; Mavros, P. Recovery of Metals by Ion Flotation from Dilute Aqueous Solutions. *Sep. Purif. Methods* **1991**, *20*, 1–48. [[CrossRef](#)]
22. Gopalratnam, V.C.; Bennett, G.F.; Peters, R.W. Effect of Collector Dosage on Metal Removal by Precipitation/Flotation. *J. Environ. Eng.* **1992**, *118*, 923–948. [[CrossRef](#)]
23. Deliyanni, E.A.; Kyzas, G.Z.; Matis, K.A. Various flotation techniques for metal ions removal. *J. Mol. Liq.* **2017**, *225*, 260–264. [[CrossRef](#)]
24. Yenial, Ü.; Bulut, G. Examination of flotation behavior of metal ions for process water remediation. *J. Mol. Liq.* **2017**, *241*, 130–135. [[CrossRef](#)]
25. Amaral Filho, J.; Azevedo, A.; Etchepare, R.; Rubio, J. Removal of sulfate ions by dissolved air flotation (DAF) following precipitation and flocculation. *Int. J. Miner. Process.* **2016**, *149*, 1–8. [[CrossRef](#)]
26. Rubio, J.; Souza, M.L.; Smith, R.W. Overview of flotation as a wastewater treatment technique. *Miner. Eng.* **2002**, *15*, 139–155. [[CrossRef](#)]
27. Capponi, F.; Sartori, M.; Souza, M.L.; Rubio, J. Modified column flotation of adsorbing iron hydroxide colloidal precipitates. *Int. J. Miner. Process.* **2006**, *79*, 167–173. [[CrossRef](#)]
28. Peleka, E.N.; Gallios, G.P.; Matis, K.A. A perspective on flotation: A review. *J. Chem. Technol. Biotechnol.* **2018**, *93*, 615–623. [[CrossRef](#)]
29. Lenter, C.M.; McDonald, L.M.; Skousen, J.G.; Ziemkiewicz, P.F. The effects of sulfate on the physical and chemical properties of actively treated acid mine drainage floc. *Mine Water Environ.* **2002**, *21*, 114–120. [[CrossRef](#)]
30. Tang, M.; Wen, S. Effects of Cations/Anions in Recycled Tailing Water on Cationic Reverse Flotation of Iron Oxides. *Minerals* **2019**, *9*, 161. [[CrossRef](#)]
31. Wu, H.; Wang, W.; Huang, Y.; Han, G.; Yang, S.; Su, S.; Sana, H.; Peng, W.; Cao, Y.; Liu, J. Comprehensive evaluation on a prospective precipitation-flotation process for metal-ions removal from wastewater simulants. *J. Hazard. Mater.* **2019**, *371*, 592–602. [[CrossRef](#)] [[PubMed](#)]
32. Wu, H.; Huang, Y.; Liu, B.; Han, G.; Su, S.; Wang, W.; Yang, S.; Xue, Y.; Li, S. An efficient separation for metal-ions from wastewater by ion precipitate flotation: Probing formation and growth evolution of metal-reagent flocs. *Chemosphere* **2021**, *263*, 128363. [[CrossRef](#)]
33. Fang, D.; Wang, Y.; Liu, H.; Zhang, H.; Ye, X.; Li, Q.; Li, J.; Wu, Z. Efficient extraction of Rb⁺ and Cs⁺ by a precipitation flotation process with ammonium phosphowolframate as precipitant. *Colloids Surf. A Physicochem. Eng. Asp.* **2021**, *608*, 125581. [[CrossRef](#)]
34. Acosta, O. *Water and Mining BT—Water Policy in Chile*; Donoso, G., Ed.; Springer: Cham, Switzerland, 2018; pp. 179–193, ISBN 978-3-319-76702-4.
35. Puigdomenech, I. *Hydra/Medusa Chemical Equilibrium Database and Plotting Software*; KTH Royal Institute of Technology: Stockholm, Sweden, 2004.
36. NMX-AA-004-SCFI-2000 Water Analysis—Determination of Settleable Solids in Natural, Wastewaters, and Wastewaters Treated—Test Method. Secretaría de Comercio y Fomento Económico, 2000.
37. Lee, G.; Bigham, J.M.; Faure, G. Removal of trace metals by coprecipitation with Fe, Al and Mn from natural waters contaminated with acid mine drainage in the Ducktown Mining District, Tennessee. *Appl. Geochem.* **2002**, *17*, 569–581. [[CrossRef](#)]
38. Zhang, L.; Wu, A.; Wang, H.; Wang, L. Representation of batch settling via fitting a logistic function. *Miner. Eng.* **2018**, *128*, 160–167. [[CrossRef](#)]
39. Seo, E.Y.; Cheong, Y.W.; Yim, G.J.; Min, K.W.; Geroni, J.N. Recovery of Fe, Al and Mn in acid coal mine drainage by sequential selective precipitation with control of pH. *Catena* **2017**, *148*, 11–16. [[CrossRef](#)]

40. Kang, X.; Xia, Z.; Wang, J.; Yang, W. A novel approach to model the batch sedimentation and estimate the settling velocity, solid volume fraction, and floc size of kaolinite in concentrated solutions. *Colloids Surf. A Physicochem. Eng. Asp.* **2019**, *579*, 123647. [[CrossRef](#)]
41. Cornell, R.M.; Giovanoli, R.; Schneider, W. Review of the hydrolysis of iron(III) and the crystallization of amorphous iron(III) hydroxide hydrate. *J. Chem. Technol. Biotechnol.* **1989**, *46*, 115–134. [[CrossRef](#)]
42. Baltpurvins, K.A.; Burns, R.C.; Lawrance, G.A.; Stuart, A.D. Effect of pH and Anion Type on the Aging of Freshly Precipitated Iron(III) Hydroxide Sludges. *Environ. Sci. Technol.* **1996**, *30*, 939–944. [[CrossRef](#)]
43. Duchoslav, J.; Steinberger, R.; Arndt, M.; Stifter, D. XPS study of zinc hydroxide as a potential corrosion product of zinc: Rapid X-ray induced conversion into zinc oxide. *Corros. Sci.* **2014**, *82*, 356–361. [[CrossRef](#)]
44. Oswald, H.R.; Asper, R. *Bivalent Metal Hydroxides BT—Preparation and Crystal Growth of Materials with Layered Structures*; Lieth, R.M.A., Ed.; Springer: Dordrecht, The Netherlands, 1977; pp. 71–140, ISBN 978-94-017-2750-1.
45. Oliveira, A.P.A. Controlled Precipitation of Zinc Oxide Particles at Room Temperature. *Chem. Mater.* **2003**, *15*, 3202–3207. [[CrossRef](#)]
46. Sánchez-Andrea, I.; Sanz, J.L.; Bijmans, M.F.M.; Stams, A.J.M. Sulfate reduction at low pH to remediate acid mine drainage. *J. Hazard. Mater.* **2014**, *269*, 98–109. [[CrossRef](#)]
47. Blais, J.; Djedidi, Z.; Cheikh, R.B.; Tyagi, R.D.; Mercier, G. Metals Precipitation from Effluents: Review. *Pract. Period. Hazard. Toxic Radioact. Waste Manag.* **2008**, *12*, 135–149. [[CrossRef](#)]
48. Noh, J.S.; Schwarz, J.A. Estimation of the point of zero charge of simple oxides by mass titration. *J. Colloid Interface Sci.* **1989**, *130*, 157–164. [[CrossRef](#)]
49. Dai, Q.; Laskowski, J.S. The Krafft point of dodecylammonium chloride: pH effect. *Langmuir* **1991**, *7*, 1361–1364. [[CrossRef](#)]
50. Smith, R.W.; Scott, J.L. Mechanisms of Dodecylamine Flotation of Quartz. *Miner. Process. Extr. Metall. Rev.* **1990**, *7*, 81–94. [[CrossRef](#)]